© 2016. Published by The Company of Biologists Ltd | Development (2016) 143, 3407-3416 doi:10.1242/dev.138602

RESEARCH ARTICLE

Jasmonate regulates juvenile-to-adult phase transition in rice

Ken-ichiro Hibara[1,§,¶], Miyako Isono[1,§], Manaki Mimura[1], Naoki Sentoku[2], Mikiko Kojima[3], Hitoshi Sakakibara[3,4], Yuka Kitomi[1,*], Takanori Yoshikawa[1,‡], Jun-ichi Itoh[1] and Yasuo Nagato[1]

ABSTRACT

Juvenile-to-adult phase transition is an important shift for the acquisition of adult vegetative characteristics and subsequent reproductive competence. We identified a recessive *precocious* (*pre*) mutant exhibiting a long leaf phenotype in rice. The long leaf phenotype is conspicuous in the second to the fourth leaves, which are juvenile and juvenile-to-adult transition leaves. We found that morphological and physiological traits, such as midrib formation, shoot meristem size, photosynthetic rate and plastochron, in juvenile and juvenile-to-adult transition stages of the *pre* mutant have precociously acquired adult characteristics. In agreement with these results, expression patterns of *miR156* and *miR172*, which are microRNAs regulating phase change, support the accelerated juvenile-to-adult phase change in the *pre* mutant. The mutated gene encodes an allene oxide synthase (OsAOS1), which is a key enzyme for the biosynthesis of jasmonic acid (JA). The *pre* mutant showed a low level of JA and enhanced sensitivity to gibberellic acid, which promotes the phase change in some plant species. We also show that prolonged plastochron in the *pre* mutant is caused by accelerated *PLASTOCHRON1* (*PLA1*) function. The present study reveals a substantial role of JA as a negative regulator of vegetative phase change.

KEY WORDS: *precocious*, Rice, Juvenile-to-adult phase transition, Jasmonic acid, ALLENE OXIDE SYNTHASE, Plastochron

INTRODUCTION

After germination, higher plants continuously produce vegetative organs, such as leaves, stems and roots, before the onset of reproductive development. The vegetative period can be divided into juvenile and adult stages, which are distinguished by changes in many physiological and morphological traits (reviewed by Poethig, 2013). It is believed that plants acquire reproductive competence during the adult stage of vegetative development.

The juvenile-to-adult phase transition is controlled by two major regulators: microRNA156 (*miR156*) and their target transcription factors, SQUAMOSA promoter-binding protein-like genes (SPLs). *miR156*, one of the most abundant microRNAs, is conserved among all land plants, including mosses (Axtell and Bowman, 2008). Recent studies have shown that *miR156* accumulation reaches the highest level in seedlings, then decreases gradually as the plant develops, resulting in a gradual increase in target *SPL* transcripts in a number of herbaceous and woody species (Wu and Poethig, 2006; Chuck et al., 2007; Wang et al., 2009, 2011; Wu et al., 2009; Tanaka et al., 2011; Yoshikawa et al., 2013; Hudson et al., 2014). Plants constitutively overexpressing *miR156* share common phenotypes in several species, for example, a prolonged juvenile phase, accelerated leaf initiation and delayed flowering (Schwab et al., 2005; Wu and Poethig, 2006; Xie et al., 2006, 2012; Zhang et al., 2011; Chuck et al., 2011). Conversely, plants with endogenous *miR156* function disrupted by mimicry targets or by T-DNA insertions exhibit opposite phenotypes, e.g. precocious adult traits (Franco-Zorrilla et al., 2007; Wu et al., 2009; Todesco et al., 2010; Yang et al., 2013; Yu et al., 2013). These results indicate that the appropriate *miR156* level is necessary and sufficient for maintenance of the juvenile phase. Genetic studies have also shown that mutants precociously exhibiting adult characteristics have low *miR156* expression, whereas mutants with an elongated juvenile phase overexpress *miR156* (Smith et al., 2009; Li et al., 2012; Chuck et al., 2007; Tanaka et al., 2011). Such studies support the importance of *miR156* levels in maintaining the juvenile phase. *miR156* induces mRNA cleavage and/or inhibits the translation of target SPLs, which are crucial transcription factors for phase transition (Wu and Poethig, 2006; Yang et al., 2012). Although *miR156* appears to be a major regulator of SPL expression and translation, recent studies have provided evidence that the expression or activity of SPLs is also regulated in a *miR156*-independent manner in response to environmental cues or the phytohormone gibberellin (Wang et al., 2009; Jung et al., 2012; Yu et al., 2012).

In addition to *miR156*, *miR172* and its target genes are thought to play important roles in juvenile-to-adult phase transition. Unlike *miR156*, *miR172* accumulation is low in the juvenile phase and then gradually increases. *miR172* acts as a repressor of APETALA2-LIKE (AP2-like) transcription factors to promote adult epidermal identity, floral development and flowering (Aukerman and Sakai, 2003; Chen, 2004; Chuck et al., 2007; Jung et al., 2007; Lauter et al., 2005; Wu et al., 2009). Plants overexpressing *miR156* have decreased *miR172* expression, whereas plants with reduced expression of *miR156* have increased levels of *miR172* (Wu et al., 2009). In *Arabidopsis*, overexpression of *miR156*-resistant *SPL9* caused an accumulation of *miR172*, which is a direct target of *SPL9*, and early flowering (Wang et al., 2009; Wu et al., 2009).

The hormone gibberellic acid (GA) is involved in vegetative phase change and regulates flowering in some plants. For example, in ivy, when the apical bud is removed from an adult branch, the subtending axillary buds will grow into typical adult branches. However, if GA is applied to the axillary buds, they will develop into juvenile branches (Rogler and Hackett, 1975; Poethig, 2013).

[1]Department of Agricultural and Environmental Biology, Graduate School of Agricultural and Life Sciences, University of Tokyo, Tokyo 113-8657, Japan. [2]Institute of Agrobiological Sciences, National Agriculture and Food Research Organization, Ibaraki 305-8602, Japan. [3]RIKEN Center for Sustainable Resource Science, Yokohama 230-0045, Japan. [4]Graduate School of Bioagricultural Sciences, Nagoya University, Nagoya 464-8601, Japan.
*Present address: Institute of Crop Science, National Agriculture and Food Research Organization, Ibaraki 305-8602, Japan. ‡Present address: School of Agricultural Regional Vitalization, Kibi International University, Hyogo 656-0484, Japan.
§These authors contributed equally to this work

¶Author for correspondence (ahibarak@mail.ecc.u-tokyo.ac.jp)

K.-i.H., 0000-0001-8578-7276

Received 13 April 2016; Accepted 4 August 2016

Development (2016) 143, 3407-3416 doi:10.1242/dev.138602

It has been also reported that GA-deficient mutants exhibit delayed transition to the adult phase in *Arabidopsis* and maize (Telfer et al., 1997; Telfer and Poethig, 1998; Evans and Poethig, 1995). Several recent studies have reported that certain DELLA proteins, which act as transcriptional repressors of the GA response, interact with and repress SPL protein activity (Yu et al., 2012). Furthermore, the GA-mediated degradation of DELLA under long-day conditions allows the SPL-mediated activation of *miR172* and floral identity genes, such as *FT* and MADS box genes, resulting in floral transition (Yu et al., 2012; Galvão et al., 2012). *miR156* expression is influenced by auxin and ethylene, and the stability of DELLAs is also regulated by several other phytohormones, including auxin, ethylene and abscisic acid (Vanstraelen and Benková, 2012; Marin et al., 2010; Zuo et al., 2012). Thus, these phytohormones might also contribute to the regulation of *miR156* and SPLs.

In rice, a number of traits are altered during the juvenile-to-adult phase transition, including the size and shape of leaf blades, the size and shape of the shoot apical meristem (SAM), the presence of midribs, plastochron, photosynthetic rate, and *miR156* and *miR172* expression levels (Asai et al., 2002; Itoh et al., 2005; Tanaka et al., 2011). Based on these observations, it is proposed that the juvenile stage comprises the first and second leaf stages, the juvenile-to-adult transition stage spans the third to fifth leaf stages, and afterwards the rice plant is considered an adult. To date, two mutants have been reported that are defective in the juvenile-to-adult phase of vegetative development in rice: *mori1* and *peter pan syndrome* (*pps*). The *mori1* mutant keeps producing second-leaf-like organs over the course of its lifetime, whereas the *pps* mutant has an extended juvenile period but shows early flowering (Asai et al., 2002; Tanaka et al., 2011). Both of these mutants show a prolonged juvenile period, but rice mutants with truncated juvenile phases have not been reported. In the present study, we describe the isolation and cloning of the *precocious* (*pre*) rice mutant, which exhibits long leaves, a shortened juvenile phase and early flowering. We show that the mutated gene (hereafter termed '*PRE*') encodes an allene oxide synthase (OsAOS1), a key enzyme in jasmonate biosynthesis. This finding suggests that jasmonate plays a substantial role in the juvenile-to-adult transition in rice.

RESULTS

Phenotype of the *pre* mutant

While screening leaf developmental mutants, we isolated a mutant exhibiting long leaves (Fig. 1A) and designated it *precocious* (*pre*), because the *pre* plant seemed to reach the adult stage precociously. Because most of the *pre* homozygous mutants withered before flowering under flooding conditions in a paddy field, *pre* mutant and wild-type plants were grown in MS medium or in pots under non-flooding conditions (see Materials and Methods). The leaf blades of *pre* were longer than those of the wild type (cv. Nipponbare) from the second to the twelfth leaves (Fig. 1B), resulting in taller plants (Fig. 1A). The leaf blade width of *pre* from the second to the ninth leaves was slightly greater than that of the wild type (Fig. 1C). To elucidate the cause of the elongated leaf blades in the *pre* mutant, we measured the length and width of epidermal cells in the second leaf blades. In the *pre* mutant, epidermal cell width was comparable to that in the wild type, whereas the length was approximately 20% greater (Fig. S1). We then estimated the number of epidermal cells in the second leaf blades by dividing the blade length and width by epidermal cell length and width, respectively, and revealed that the epidermal cell number in *pre* was greater by approximately 70% in the direction of length and 25% in the direction of width (Fig. 1D). These results indicate that the greater leaf size in the *pre* mutant is mainly caused by the increase in cell number, although cell elongation is also involved.

The 'long leaf' phenotype was more conspicuous in the second to the fourth leaves than in the upper leaves (Fig. 1E). This suggests that juvenile and juvenile-to-adult transition leaves (second-fourth leaves) may have precociously acquired adult characteristics in *pre* plants, resulting in a shortened juvenile phase. We next examined juvenility-related characteristics in the *pre* mutant. The midrib is a clear morphological marker distinguishing juvenile and adult leaves; it is almost absent in juvenile leaves (second leaf) but present in approximately 50% and over 70% of the blade length in the third leaf and adult leaves, respectively, in wild type (Asai et al., 2002; Tanaka et al., 2011; Fig. 1F; Fig. S2). In *pre* plants, midribs in the second and third leaf blades were formed in approximately 22% and 60% of the total leaf blade length, respectively (Fig. 1F; Fig. S2). These values were greater than those of the wild type (~7% and 50%, respectively). This result supports the notion that *pre* second and third leaves precociously express adult characteristics.

Other morphological and physiological traits that differ between the juvenile and adult phases in rice (Itoh et al., 2005) also supported this idea. The wild-type SAM gradually becomes enlarged during plant development. We compared the SAM width at the second to fifth leaf stages between the *pre* mutant and the wild type. The width of the SAM in *pre* plants was almost equal to that in the wild type during the second leaf stage; however, the width was consistently larger than that in the wild type after the third leaf stage (Fig. 1G). The physiological traits associated with the phase transition showed the same tendency. Generally, in wild-type plants, the photosynthetic rate is low in juvenile leaves (the second leaves) and then increases gradually in juvenile-to-adult transition leaves (the third to fifth leaves) (Asai et al., 2002; Tanaka et al., 2011). In the wild type, the photosynthetic rate reaches its peak during the fourth leaf stage (Fig. 1H). By contrast, the *pre* mutant reached its maximum photosynthetic rate as early as the third leaf stage (Fig. 1H). We measured the plastochron (the period between the initiation of two successive leaves), which was shorter in the juvenile phase than in the adult phase. After the third week post-sowing, *pre* plants consistently produced fewer leaves than did the wild type by approximately one leaf throughout the vegetative phase (Fig. 1I). This indicated that *pre* mutants had the same plastochron as the wild type during the adult vegetative phase and that the reduction in leaf production rate took place transiently after the first week post-sowing. All of the data described above support the idea that the mutation in *PRE* accelerates the appearance of adult traits in leaf length, midrib formation, SAM size, photosynthesis rate, and plastochron.

We next examined the reproductive phenotypes of the *pre* mutant. The *pre* mutant flowered approximately 5 days earlier than did the wild type (Fig. 1J). At the heading, the total number of leaves in wild type was 15 on average, and that in the *pre* mutant was 14.3 ($n \geq 12$). Although the juvenile-to-adult phase transition occurred early in the *pre* mutant, the duration of the adult phase should be unaffected. In wild-type flowers (florets), swelling of lodicules causes flower opening, and their withering causes flower closing soon after flowering (Fig. 1K). By contrast, the flowers of *pre* plants remained open after flowering (Fig. 1L) owing to their non-withering lodicules (Fig. 1M). Furthermore, *pre* flowers rarely set seeds. Thus, *PRE* is also associated with the function of lodicules and seed formation.

Development (2016) 143, 3407-3416 doi:10.1242/dev.138602

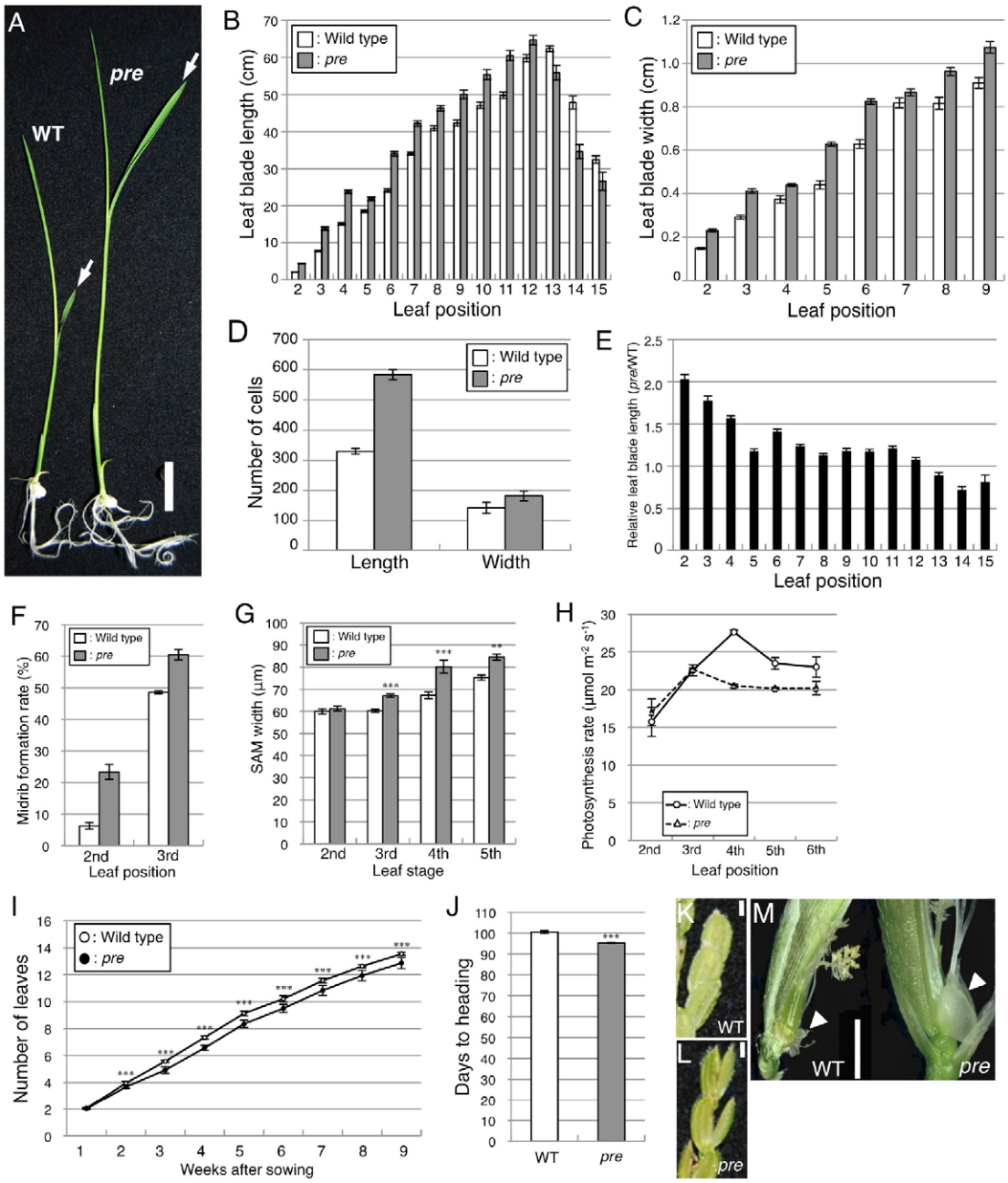

Fig. 1. Phenotypes of the *pre* mutant. (A) Wild-type (WT; left) and *pre* mutant (right) plants at 7 days after germination. Arrows indicate the second leaves. (B,C) Change of leaf blade length (B) and width (C) with leaf positions in wild-type and *pre* mutant plants (n=12). (D) Number of epidermal cells in the second leaf blade of wild-type and *pre* mutant plants. The number of cells was estimated by dividing the width and length of the leaf blade by those of epidermal cells, respectively (n=5). (E) Leaf blade length of the *pre* mutant relative to that of wild type in each leaf position. Each value was calculated from the data in C. (F) The percentage of midrib length out of total length in second and third leaf blades (n≥3). (G) Width of shoot apical meristem at each leaf stage (n=5). (H) Photosynthetic rates in wild-type and *pre* mutant leaves (n=3). (I) Increase in the number of leaves in wild type and the *pre* mutant after sowing (n=12). (J) Days to heading from sowing in wild type and the *pre* mutant (n≥12). (K,L) Flower phenotype about 1 week after opening in wild type (K) and the *pre* mutant (L). (M) Flowers about 1 day after opening. Lodicule in wild type (left) has withered, whereas that of the *pre* mutant (right) remains swollen. Arrowheads indicate lodicules. Scale bars: 1 cm (A); 2 mm (K-M). Data are shown as mean±s.e.m. (B-H) or mean±s.d. (I,J). **P<0.01, ***P<0.001 (Student's t-test).

Gene expression related to the juvenile-to-adult phase transition

Recently, *miR156* and *miR172* have been reported as molecular markers for the juvenile-to-adult phase transition in several plant species: the expression level of *miR156* is high during the juvenile phase and downregulated during the adult phase, whereas *miR172* expression follows the opposite pattern (Aukerman and Sakai, 2003; Chuck et al., 2007; Lauter et al., 2005; Tanaka et al., 2011; Wu and Poethig, 2006; Yoshikawa et al., 2013). Similarly, in rice, the expression level of *miR156* was highest in the second leaf and then declined, whereas *miR172* expression was repressed in the second leaf but increased with development (as previously reported; see Tanaka et al., 2011; Fig. 2). The expression of *miR156* in *pre* plants was, however, consistently low from the second leaf onwards, and *miR172* expression was high as early as the third leaf (Fig. 2). Precocious downregulation of *miR156* and upregulation of *miR172*

Development (2016) 143, 3407-3416 doi:10.1242/dev.138602

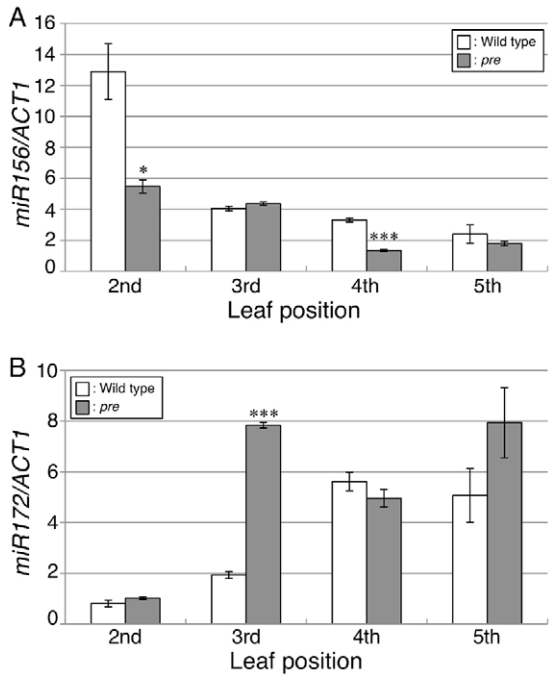

Fig. 2. Expression of *miR156* and *miR172*. (A,B) Relative expression level determined by qRT-PCR analysis of *miR156* (A) and *miR172* (B) in wild-type and *pre* leaves. Each expression level was normalized to that of *OsACTIN1*. The data shown are means of three biological replicates ±s.e.m. **P*<0.05, ****P*<0.001 (Student's *t*-test).

in *pre* plants during the early stages, together with the results of morphological and physiological analyses, signifies an accelerated juvenile-to-adult phase transition.

Identification of the *PRE* gene and its expression patterns

We employed a map-based cloning approach to isolate the *PRE* gene from F2 plants derived from the cross between *pre* heterozygotes and Kasalath (*indica* variety). The *PRE* locus was mapped to the long arm of chromosome 3 around 143 cM (Fig. 3A). We compared the nucleotide sequences of 25 candidate genes in this region between *pre* and the wild type and found only one difference, a 33-nucleotide deletion in *pre* (Fig. 3B). This deletion influenced two transcripts, *Os03t0767000-01* and *Os03t0766900-02* (Fig. 3B). Os03t0767000-01 protein derived from the *Os03g0767000* locus was truncated by 11 amino acids, whereas 33 bp were deleted from the 3′-untranslated region of *Os03t0766900-02*. Semi-quantitative reverse transcription (RT)-PCR analysis revealed that the expression levels of these genes in the *pre* mutant showed no striking change (Fig. 3C), suggesting that this deletion might have little impact on the stability of these transcripts. As the *pre* mutation seemed to impair Os03g0767000 protein activity, we introduced a 6.0-kb genomic DNA fragment containing the entire *Os03g0767000* open reading frame (ORF) without the *Os03g0766900* ORF into the *pre* mutant. The transformed plants complemented *pre* phenotypes in leaf blades and flowers (Fig. 3D,E). Thus, *Os03g0767000* is the gene responsible for the *pre* phenotype.

Os03g0767000 consists of one exon comprising 1539 nucleotides and encodes a protein of 513 amino acid residues with three conserved domains: an I-helix, a heme-binding site and a chloroplast transit peptide (Haga and Iino, 2004). These domains are the consensus sequences for ALLENE OXIDE SYNTHASE (AOS), a key enzyme for the biosynthesis of jasmonic acid (JA), which catalyzes the conversion of 13-HPOT [13*S*-hydroperoxy-(9*Z*,11*E*,15)-octadecatrienoic acid] to 12,13-EOT [(9*Z*,13*S*,15*Z*)-12,13-oxido-9,11,15-octadecatrienoic acid]. The amino acid sequences encoded by the deleted 33-bp region in the *pre* mutant were widely conserved among several plant species (Fig. S3A). Four *AOS* genes were predicted in the rice genome, and *PRE* encodes OsAOS1 (Haga and Iino, 2004; Fig. S3B). *OsAOS1* is expressed predominantly in seedlings, whereas the other three paralogs are expressed mainly in roots at a low level compared with *OsAOS1* (based on data retrieved from RiceXPro: http://ricexpro.dna.affrc.go.jp) (Haga and Iino, 2004; Sato et al., 2011). Furthermore, endogenous JA content was significantly lower in *pre* plants (Fig. 3F). Therefore, *PRE/OsAOS1* plays essential roles in JA biosynthesis and the juvenile-to-adult phase transition.

We performed qRT-PCR analysis to elucidate the patterns of *PRE* expression. Expression of *PRE* was high in ovaries at 2 days after pollination (DAP) and in mature leaf sheaths and blades (Fig. S4). To characterize the spatial expression patterns of *PRE* in detail, we carried out *in situ* hybridization. In the shoot apex, signals were not detected in SAM or P1 leaf primordium, but strong signals were detected in stem and P3 to P5 leaf sheaths (Fig. 4A) and in the boundary region between the leaf sheaths and blades of P2 and P3 leaf primordia (Fig. 4B). Strong expression was also detected in the bundle sheath extension of P3 and P4 leaf sheaths and vasculature (Fig. 4C,D) and in the ground meristem adjacent to the peripheral cylinder of vascular bundles from which the crown root initiated (Fig. 4E). In young inflorescences, *PRE* mRNA was observed in the meristem and vasculature (Fig. 4F). All floral organs, including glumes, seemed to express *PRE*, but signals were particularly strong in the stamens and vasculature (Fig. 4G). In 2 DAP ovaries, signals were detected in the embryo, endosperm and vasculature of the ovary wall (Fig. 4H). When *in situ* hybridization was performed using the *PRE* sense probe, signals were detected in a patchy pattern in leaf primordia (Fig. S5). This expression pattern would reflect that of *Os03t0766900-02*, because the *PRE* ORF overlapped with the 3′-UTR of the *Os03t0766900-02* transcript in the reverse direction (Fig. 3B).

Hormonal responses in the *pre* mutant

We examined whether the application of exogenous methyl jasmonate (MeJA) could counteract the *pre* defects. In the second leaf of the wild type, growth of both leaf blades and sheaths was suppressed in a dose-responsive manner (Fig. 5A). A marked dose-responsive reduction occurred in *pre* leaves, and the second leaf blade length of the *pre* mutant became nearly equal to that of the wild type when more than 10^{-8} M MeJA was applied (Fig. 5A,B). In addition, wild-type seedlings grown on medium containing MeJA exhibited short leaf blades and a decline in the rate of midrib formation in third leaf blade (Fig. S6). This result is opposite to that in the *pre* mutant grown on JA-free conditions, suggesting that exogenous JA extends the period of the juvenile phase.

Next, we examined the GA response in *pre* mutants. GA is reported to promote the juvenile-to-adult phase transition; the GA-deficient mutant *ga1-3* failed to transit to the adult phase in *Arabidopsis*, and the *dwarf* mutant in maize showed a prolonged juvenile phase owing to low GA content (Evans and Poethig, 1995; Telfer et al., 1997). It has also been reported that the GA signaling repressor DELLA binds directly to the JA signaling repressor JAZ, signifying an interaction between GA and JA (Hou et al., 2010). To evaluate GA sensitivity, we examined the effect of GA application on the growth of second leaf blades. Leaf blade growth was more enhanced in *pre* plants than in the wild type when more than 10^{-7} M

Development (2016) 143, 3407-3416 doi:10.1242/dev.138602

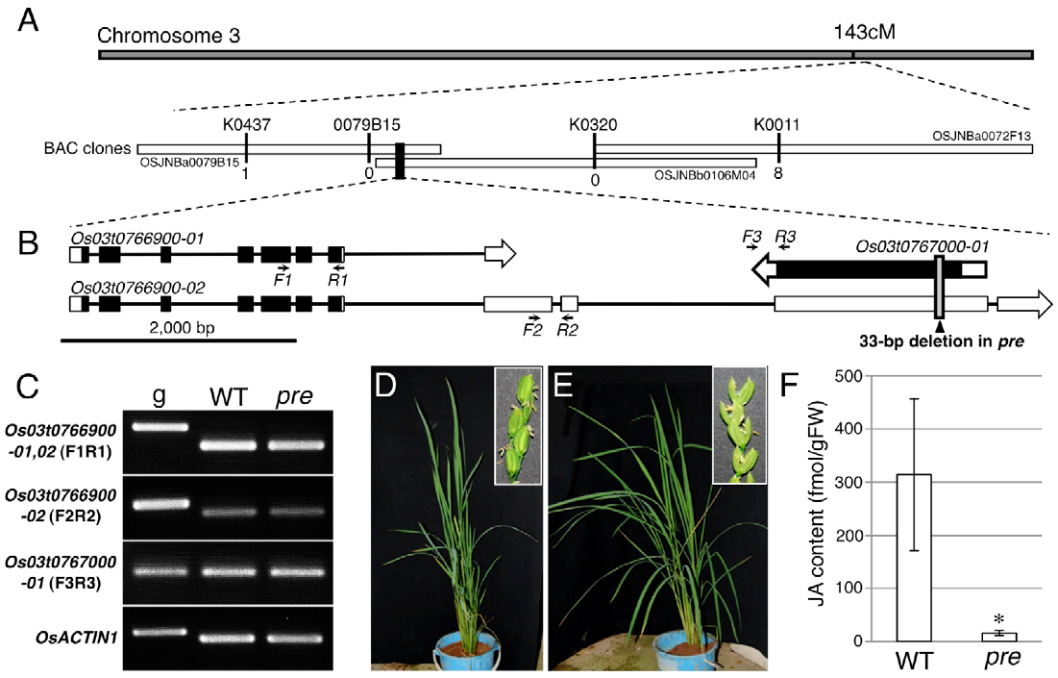

Fig. 3. Isolation of the *PRE* gene. (A) Mapped position of *PRE*. The numbers of recombinants are given below the vertical bars representing markers (K0437, 0079B015, K0320, K0011). (B) Representative transcripts around the deletion site in *pre*. Gray vertical bar shows the 33-bp deletion site in *pre*. White and black boxes represent untranslated regions and the open reading frames, respectively. Horizontal lines indicate introns. Small arrows (F1, F2, F3, R1, R2 and R3) indicate primers used for the semi-quantitative RT-PCR shown in C. (C) Semi-quantitative RT-PCR analysis of representative transcripts in 7-day-old shoot apex in wild type (WT) and the *pre* mutant. Genomic DNA (g) was used as a positive control reaction. Note that the primer pair (F1R1) for the detection of the *Os03t0766900-01* transcript can also amplify the *Os03t0766900-02* transcript. *OsACTIN1* was used as internal control. (D,E) Complementation test. The *pre* mutant was transformed with a 6.0-kb genomic fragment including the *Os03g0767000* ORF (D) or with empty vector (E). Insets in D and E show flower phenotype in each plant. (F) Endogenous JA content in wild-type and *pre* 7-day-old seedlings. Values are shown as means of three biological replications ±s.e.m. gFW, grams fresh weight. **P*<0.05 (Student's *t*-test).

GA was applied (Fig. 5C). Thus, the precocious juvenile-to-adult phase transition in *pre* mutants might be caused by a reduction in JA content and enhanced sensitivity to GA.

Relationship between PRE and the plastochron-regulating factors PLA1 and PLA2

The *pre* mutant transiently exhibited a prolonged plastochron during the juvenile-to-adult transition stage (Fig. 1I). This phenotype contrasts with those of *pla1* and *pla2* mutants, which have short plastochrons (Itoh et al., 1998; Miyoshi et al., 2004; Kawakatsu et al., 2006). *PLA1* and *PLA2* encode a cytochrome P450 protein, CYP78A11, and an RNA-binding protein, respectively (Miyoshi et al., 2004; Kawakatsu et al., 2006). Hence, it is possible that overexpression of *PLA1* and/or *PLA2* may partly recreate the *pre* phenotype. qRT-PCR analysis revealed that *PLA1* expression was upregulated in *pre* plants, whereas that of *PLA2* was not affected (Fig. 6A). *PLA1* expression in *pre* plants did not alter its specific localization (Fig. S7). Next, we generated the *PLA1-High Copy* (*PLA1-HC*) line by introducing a 6.0-kb *PLA1* genomic fragment into the wild type, in which *PLA1* expression was increased more than fivefold (Fig. S8). *PLA1-HC* plants exhibited lengthened plastochrons and long leaves (Fig. 6B-D). These results suggest that the *pre* phenotype is partly mediated by enhanced *PLA1* expression.

To investigate the relationship between *PRE* and *PLA1* further, we generated the *pre pla1* double mutant (Fig. 6E) and measured plastochron and leaf blade length each week (Fig. 6F,G). As shown in Fig. 1I, leaf number in 2- to 4-week-old plants was lower in the *pre* mutant than in the wild type. The *pre pla1* double mutant showed short plastochrons, comparable to those of *pla1* plants (Fig. 6F). Leaf blades of *pre pla1* double mutants, however, were significantly longer than those of *pla1* mutants at all leaf positions examined, although much shorter than those of *pre* plants (Fig. 6G). These results suggest that *PRE* might be involved in plastochron regulation via *PLA1*, but that *PRE* and *PLA1* act independently in the regulation of leaf blade length.

We also generated the *pre pla2* double mutant (Fig. 6H). Unlike *pre pla1* plants, leaf number in 2- to 5-week-old *pre pla2* plants was significantly lower than that of *pla2* plants, although it was significantly higher than that of wild type (Fig. 6I). The leaf blade of *pre pla2* plants was also significantly longer than that of *pla2* plants (Fig. 6J). Thus, *PRE* and *PLA2* may function independently in both plastochron and leaf blade length regulation.

DISCUSSION

JA plays a substantial role in the juvenile-to-adult phase transition in rice

In this study, we revealed that the *pre* mutant exhibited long leaves and a precocious transition from juvenile to adult owing to a loss-of-function mutation in the allene oxide synthase gene *OsAOS1*. To date, JA and its various metabolites regulate plant responses to abiotic and biotic stresses, as well as plant growth and developmental processes, including senescence, tendril coiling, leaf abscission, tuber formation and inflorescence and flower development (reviewed by Santino et al., 2013; Yuan and Zhang, 2015). The *pre* mutant exhibited not only defects related to the juvenile-to-adult phase change but also withering in flooding conditions and defects in flower closing and fertilization. Withering in flooding conditions might reflect diminished tolerance against

Development (2016) 143, 3407-3416 doi:10.1242/dev.138602

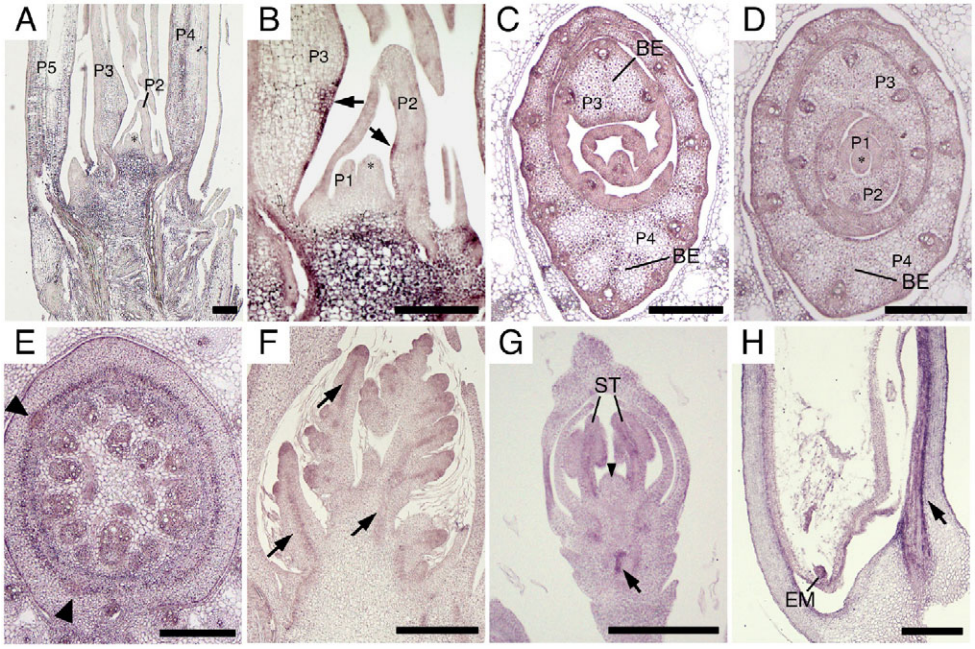

Fig. 4. *In situ* hybridization analysis of *PRE* expression. (A) Longitudinal section of shoot apex in a 10-day-old seedling. (B) Magnified view of shoot apex from A. Arrows indicate the boundary region between the leaf sheath and blade. (C-E) Cross-sections of leaf sheath (C), shoot apex (D) and stem (E) in a 7-day-old seedling. Asterisks in A,B,D indicate shoot apical meristems. Arrowheads in E indicate crown root primordia. P1 to P5 indicate stages of leaf primordia. (F) An immature panicle at elongation stage of primary branches. (G) Longitudinal section of flower. Arrowhead indicates floral meristem. (H) Developing seed at 2 days after pollination. Arrows in F-H indicate vasculatures. BE, bundle sheath extension; EM, embryo; ST, stamen. Scale bars: 200 µm (A-F); 100 µm (G,H).

abiotic stress. Sterile phenotype is consistent with other reports in which most of the mutants defective in JA biosynthesis show male sterility (Ishiguro et al., 2001; von Malek et al., 2002; Park et al., 2002; Caldelari et al., 2011; Yuan and Zhang, 2015).

JA controls leaf growth by negatively affecting cell cycle progression and endoreduplication in a *COI1*-dependent manner in *Arabidopsis* (Noir et al., 2013). In rice, it has been reported that a *cpm2* (*coleoptile photomorphogenesis2*)/*hebiba* mutant defective in allene oxide cyclase (AOC) and an *eg1* (*extra glume1*) mutant defective in a lipase involved in JA biosynthesis have longer leaves (Riemann et al., 2003, 2013; Cai et al., 2014). Similarly, the longer leaf phenotype of the *pre* mutant was caused by increased cellular proliferation rather than cellular expansion (Fig. 1D). Thus, JA-related mutants exhibit long leaves in both dicots and monocots, although this phenotype has not been discussed in relation to the juvenile-to-adult phase transition.

The *pre* mutant showed abnormal morphological and physiological phenotypes other than long leaves, all of which indicated that juvenile (second leaf) and juvenile-to-adult transition (third to fifth leaves) leaves appear more adult than those of the wild type. The expression of two microRNAs (*miR156* and *miR172*), known as molecular markers for the juvenile-to-adult phase transition (Poethig, 2013), supports the hypothesis that *pre* mutants underwent a precocious phase transition. Other JA-related mutants of rice (*cpm1*, *cpm2* and *eg1*) also have long leaves (Haga and Iino, 2004; Riemann et al., 2003; Cai et al., 2014), but phase transition-related traits have not been examined. Based on phenotypic similarities, these mutations may also affect the juvenile-to-adult phase transition.

Based on the results of clonal analysis and shoot apex culture of maize, Orkwiszewski and Poethig (2000) argued that vegetative phase identity is determined after leaf initiation, and factors driving phase transition do not originate in the SAM. *PPS* is also expressed strongly in the fourth and fifth leaves, but not in the SAM (Tanaka et al., 2011). The present results, which revealed strong expression of *PRE* (*OsAOS1*) in the leaf sheath, stem and young leaf primordia, but not in the SAM (Fig. 4; Fig. S4), support the hypothesis that the initial step of the vegetative phase transition occurs in leaves.

Several mutants with truncated juvenile phases have been reported in some plant species. The *zip* (*zippy*) mutant in *Arabidopsis* produced first and second leaves with adult characteristics, i.e. serrate and narrow leaves with abaxial

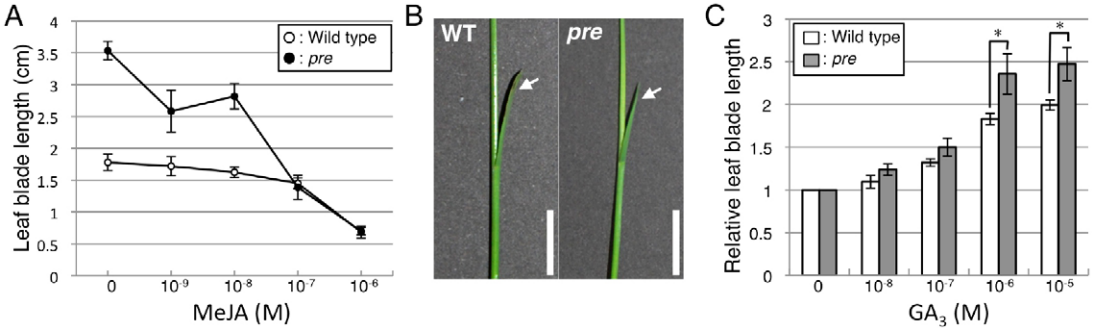

Fig. 5. Effect of JA and GA on leaf blade growth of *pre* mutants. (A) The second leaf blade length of wild type and *pre* mutants 11 days after germination on medium containing different concentrations of MeJA ($n \geq 3$). Data are shown as mean±s.e.m. (B) The second leaf blades (arrows) of wild-type (WT) and *pre* plants germinated on the medium containing 10^{-7} M MeJA. Scale bars: 1 cm. (C) Relative leaf blade length of wild type and *pre* mutants 11 days after germination on medium containing different concentrations of GA_3 ($n \geq 3$). Data are shown as means of values relative to that when 0 M GA_3 was applied ±s.e.m. *$P<0.05$ (Student's *t*-test).

Development (2016) 143, 3407-3416 doi:10.1242/dev.138602

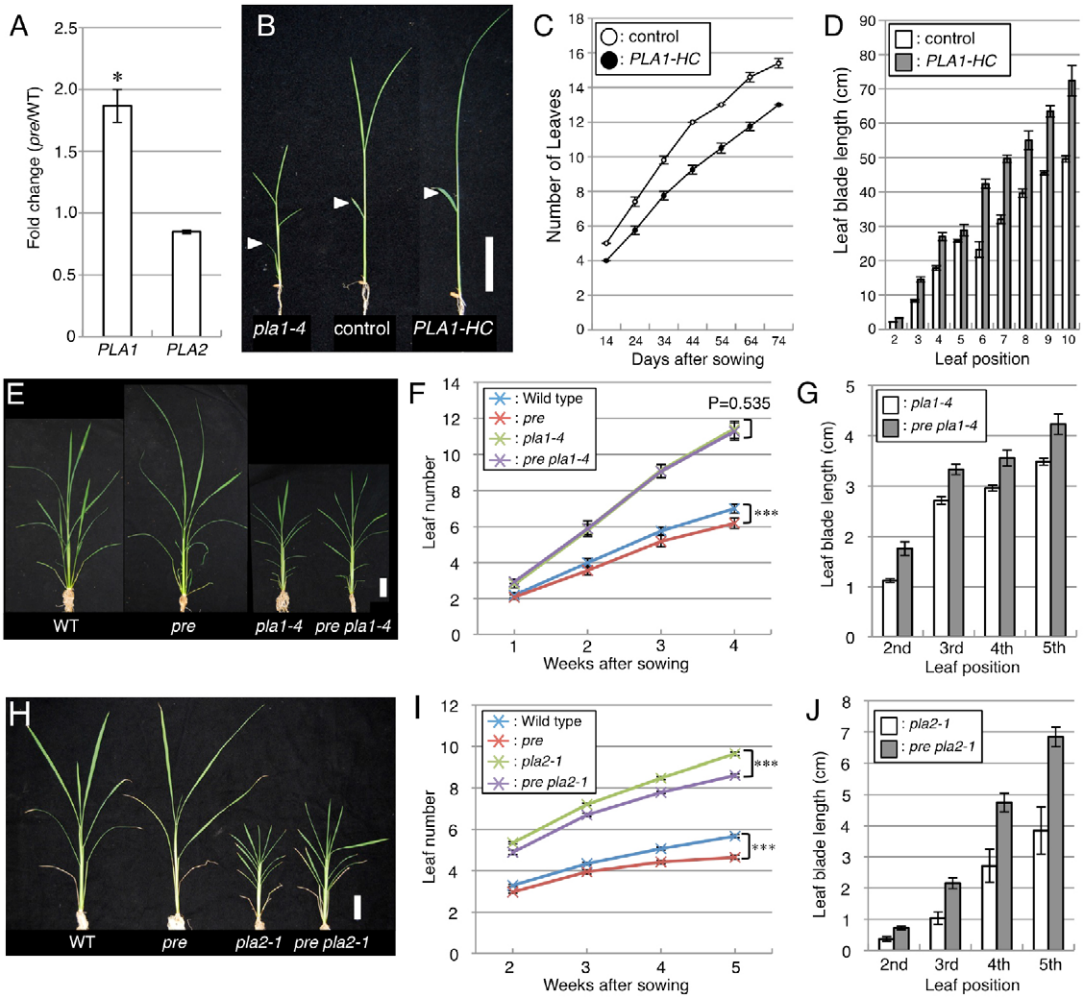

Fig. 6. Relationships between *PRE* and *PLA* genes. (A) Expression levels of *PLA1* and *PLA2* in the *pre* mutant relative to that in wild type. One-week-old shoot apices were used. The data were derived from three biological replicates. Each expression level was normalized by that of *OsACTIN1*. Error bars represent s.d. **P*<0.05 (Student's *t*-test). (B) A *pla1-4* plant, a control (wild-type) plant transformed with empty vector and a *PLA1-HC* plant 2 weeks after sowing. Arrowheads indicate second leaves. (C) Increase in the number of leaves after sowing in control and *PLA1-HC* plants ($n \geq 4$). (D) Leaf blade length in control and *PLA1-HC* plants ($n \geq 4$). (E) Wild-type, *pre*, *pla1-4* and *pre pla1-4* plants 35 days after sowing. (F) Increase in the number of leaves after sowing in wild-type, *pre*, *pla1-4* and *pre pla1-4* plants. (G) Change of leaf blade length with leaf positions in *pla1-4* and *pre pla1-4* plants ($n \geq 10$). (H) Wild-type, *pre*, *pla2-1* and *pre pla2-1* plants 49 days after sowing. (I) Increase in the number of leaves after sowing in wild-type, *pre*, *pla2-1* and *pre pla2-1* plants. (J) Change of leaf blade length with leaf positions in *pla2-1* and *pre pla2-1* plants ($n \geq 10$). Scale bars: 5 cm (B,E,H). Data in C,D,F,G,I,J are shown as mean±s.e.m. ****P*<0.001 (Student's *t*-test).

trichomes (Hunter et al., 2003). Also, the *zip* mutant showed an accumulation of *SPL3* transcripts, which is one of the targets of *miR156* (Wu and Poethig, 2006). The maize *glossy15* mutant showed an accelerated phase transition only in leaf epidermal cells (epicuticular wax composition, cell wall characteristics and the existence of differentiated epidermal macrohairs and bulliform cells), but other traits involved in phase transition appeared normal (Moose and Sisco, 1994). Thus, among heterochronic mutants, some may affect only specific organs/tissues. The *pre* mutant displayed abnormalities in all traits examined, indicating an upstream role for *PRE* and/or JA in the juvenile-to-adult phase transition cascade.

The heading date of *pre* plants was approximately 5 days earlier than that of the wild type (Fig. 1J). Considering that the *pre* juvenile period was truncated by one plastochron (~5 days), the duration of the adult period is considered to be unaffected. A similar phenomenon is observed in *Arabidopsis hasty*, in which both juvenile-to-adult phase transition and floral induction were accelerated (Bollman et al., 2003). Conversely, the rice *pps* mutant exhibited a retarded vegetative phase transition but early heading, resulting in a truncated adult phase (Tanaka et al., 2011). Because *PPS* is an *Arabidopsis COP1* ortholog that has pleiotropic functions on development, *PPS* function in reproductive transition should be independent of that in vegetative transition. Considering cases of various heterochronic mutants, the timing of juvenile-to-adult phase transitions is not expected to affect the timing of the reproductive phase transition directly.

Relationship between GA and JA in phase transition

The phytohormone GA is a positive factor for vegetative phase transition in several plant species (Evans and Poethig, 1995; Telfer et al., 1997; Tanaka et al., 2011). The present results indicate that JA is a negative factor for the vegetative phase transition. In *Arabidopsis*, GA and JA are antagonistic in developmental events such as hypocotyl elongation, root growth, flowering and defense responses via an interaction between DELLA and JAZ proteins (Navarro et al., 2008; Hou et al., 2010; Wild et al., 2012). Furthermore, in rice, GA application caused leaf expansion whereas

Development (2016) 143, 3407-3416 doi:10.1242/dev.138602

JA application reduced leaf size (Fig. 5A), suggesting that the antagonistic relationship between JA and GA (and also between DELLA and JAZ) is retained in rice.

pre leaf blades showed hypersensitivity to GA when more than 10^{-7} M GA_3 was used (Fig. 5C), raising the possibility that the change in susceptibility to GA in the *pre* mutant influenced the timing of the juvenile-to-adult phase transition. It is interesting to consider whether enhanced tissue-specific GA responsiveness associated with reduced JA content, or JA signaling directly, is responsible for the precocious transition to adult phase.

Relationship between JA and *PLA* genes on the plastochron and leaf growth

Expression analyses by qRT-PCR and *in situ* hybridization indicated that *PRE* quantitatively, but not spatially, regulated *PLA1* expression, resulting in the prolonged plastochron in *pre* (Fig. 6F). However, the regulation of leaf blade length by *PRE* was independent of that by *PLA1* (Fig. 6G). Based on these results, the phenotype of *pre pla1* double mutants may be interpreted as follows: both *pla1* and *pre pla1* plants exhibited similar plastochrons owing to the loss of function of *PLA1*, but leaf blade length was greater for *pre pla1* than for *pla1* plants, because *PRE* and/or JA contents regulate plastochron via *PLA1* function during early stage and leaf blade length independently of *PLA1*.

The relationship between *PRE* and *PLA2* differs from that between *PRE* and *PLA1*. Both plastochrons and lead blades of *pre pla2* plants were longer than those of *pla2* plants, suggesting that *PRE* is independent of the *PLA2* pathway. In accordance with this result, *PLA1* was upregulated in *pre* mutants, but *PLA2* was not (Fig. 6A). Kawakatsu et al. (2006) reported that *PLA1* and *PLA2* act in independent pathways regulating leaf maturation, plastochrons and the duration of the vegetative phase. In addition, GA promoted *PLA1* and *PLA2* expression, and the GA inhibitor uniconazole suppressed their expression (Mimura et al., 2012).

As described above, the relationships among *PRE*, *PLA1*, *PLA2*, JA and GA are highly complex. *PRE*-mediated JA content and GA play substantial roles in the vegetative phase transition. Although the roles of *PLA1* and *PLA2* in phase transition have not been described explicitly, the regulation of *PLA1* expression by *PRE* suggests that *PLA1* is a phase transition regulator.

In the present study, we examined the *pre* mutant in detail and revealed that it underwent a precocious phase transition. Identification of the causal gene revealed a substantial role for JA as a negative regulator of the vegetative phase transition in rice. Recently, Beydler et al. have reported that genes related to stress response pathways, such as jasmonic acid, are upregulated in juvenile leaf primordia and exogenous JA application delays the emergence of adult traits in maize (Beydler et al., 2016). Additional studies will be required to determine how JA has an impact on vegetative phase transition and to examine the relationship between the stress response and developmental phase change.

MATERIALS AND METHODS

Plant materials and growth conditions

The *pre* mutant was obtained from the population of Tos17 insertion lines of cv. Nipponbare (Hirochika, 2001; Hirochika et al., 1996). *pla1-4* and *pla2-1* mutants were reported in previous works (Miyoshi et al., 2004; Kawakatsu et al., 2006). These mutations were maintained in a heterozygous state. For double mutant analysis, wild type, each single mutant, *pre pla1-4* and *pre pla2-1* double mutants generated from double heterozygous plants were identified by PCR-based genotyping. In a paddy field, most of the *pre* homozygous plants died before heading. For that reason, *pre* mutant and wild-type plants were grown in MS medium (Murashige and Skoog, 1962) containing 3% sucrose and 1% agar at 28°C under continuous light conditions or in pots under non-flooding conditions. Transgenic plants were grown in a biohazard greenhouse at 30°C in the daytime and 25°C at night.

Histological analysis

For paraffin-embedded sections, samples were fixed in formaldehyde-acetic acid solution (formaldehyde:glacial acetic acid:ethanol=2:1:17) for 24 h at 4°C. They were dehydrated in a graded ethanol series, and embedded in Paraplast plus (McCormick Scientific). Microtome sections (8 µm thick) were stained with Delafield's Hematoxylin and observed with a light microscope.

Measurement of photosynthetic rate

For measuring photosynthetic rate, fully expanded second to sixth leaf blades of the wild type and *pre* mutant were used. Rates of photosynthetic CO_2 assimilation were measured using a portable gas exchange system (LI-6400; Li-Cor). Measurements were replicated for three plants. Light was provided by an LED source (red/blue, 6400-02 LED source; Li-Cor). During the measurement of photosynthetic CO_2 assimilation rates, the photon flux density was 1300 µmol/m^2s, leaf temperature was 25°C, and the reference CO_2 concentration was 370 ml/l.

RT-PCR analysis

Total RNA was extracted using TRIzol reagent (Invitrogen) or RNeasy (Qiagen) according to the manufacturer's instructions. The reverse transcriptional reaction was performed using High Capacity cDNA Reverse Transcription Kits (Applied Biosystems) according to the manufacturer's instructions. To quantify gene expression, qRT-PCR analysis of *PLA1*, *PLA2* and *OsACTIN1* (*ACT1*) was performed using the TaqMan Fast Universal PCR Master Mix (Applied Biosystems) and FAM-labeled TaqMan probes for each gene, and qRT-PCR analysis of *miR156* and *miR172* was performed using TaqMan MicroRNA Assays (Applied Biosystems), on a StepOnePlus real-time PCR system (Applied Biosystems). The primers for *ACT1* were 5′-GCTATGTACGTCGCCATCCA-3′ and 5′-GCTGACACCATCACCAGAGT-3′, and the TaqMan probe was 5′-CAATACCTGTGGTACGACCACTGGCATACAG-3′ including FAM dye at the 5′-end and BQH1 at the 3′-end. The primers and TaqMan probes for *PLA1* and *PLA2* were prepared as described by Mimura et al. (2012). For RT-PCR, RNA extraction was performed as described above. Reverse-transcribed cDNA was synthesized from 1 µg of total RNA using Superscript III reverse transcriptase (Invitrogen). The primers for RT-PCR are listed in Table S1.

Map-based cloning

To map the *PRE* locus, *pre* heterozygous plants (*O. sativa* L. ssp. *japonica*) were crossed with cv. Kasalath (ssp. *indica*), and siblings with longer leaf blades were used for calculating recombination between the mutation site and PCR-based polymorphic markers. The *PRE* locus was mapped onto the long arm of chromosome 3 using STS markers obtained from the rice genome database (http://rgp.dna.affrc.go.jp/E/publicdata/caps/index.html). Further fine-mapping limited the *PRE* locus around 143 cM between two markers (K0437 and K0011). Primers for fine-mapping of *pre* are listed in Table S1. To define the molecular lesion in the *pre* mutation, the candidate genes were amplified via PCR from both *pre* and wild-type genomic DNAs, and these PCR products were sequenced.

Transgenic plants

For the complementation test, a 6.0-kb *PRE* genomic fragment, including 2.0 kb upstream and 2.0 kb downstream, was ligated to an *Agrobacterium* binary vector, pPZP2H-lac. The *PRE* gene construct was introduced into *Agrobacterium tumefaciens* strain EHA105 and transformed into *pre* mutant calli by the *Agrobacterium*-mediated transformation method (Ozawa, 2012). As a control, the pPZP2H-lac empty vector was also transformed into *pre* mutant calli. For construction of the overexpressing *PLA1* line, a pBGH/P450 vector including a *PLA1* genomic fragment (Miyoshi et al., 2004) was introduced into wild type (cv. Taichung 65). As a control, the pPZP2H-lac empty vector was also transformed into wild type.

Development (2016) 143, 3407-3416 doi:10.1242/dev.138602

In situ hybridization

Samples were fixed in 4% (w/v) paraformaldehyde and 1% Triton X-100 in 0.1 M sodium phosphate buffer for 48 h at 4°C, dehydrated in a graded ethanol series, and embedded in Paraplast plus (McCormick Scientific). Paraffin sections (8 µm thick) were applied to microscope slides coated with MAS (Matsunami Glass). The *PRE* antisense probe was prepared from the coding regions without the poly(A) region. Digoxigenin (DIG)-labeled antisense and sense RNA probes were generated by *in vitro* transcription with T7 RNA polymerase and DIG-RNA labeling mix (Roche). *In situ* hybridization and immunological detection of the hybridization signals were carried out as described by Kouchi and Hata (1993).

Jasmonic acid and gibberellin treatment

Wild-type and mutant seeds were sterilized with 3% NaClO for 25 min, and washed four times in sterile distilled water. The seeds were then placed on MS medium containing various concentrations of MeJA (methyl jasmonate; WAKO) or GA_3 (gibberellin A_3; WAKO). Plants were grown in a growth chamber under continuous light at 28°C. After 11 days, the second or third leaf blade and sheath length were measured for more than five plants in each treatment.

Jasmonate measurement

Sampling of approximately 100 mg of fresh whole shoot samples from 7-day-old seedlings (same as the seedlings in Fig. 1A) was repeated three times for both *pre* mutants and the wild type. Extraction and determination of JA in each sample were performed using a liquid chromatography-tandem mass spectrometry system (AQUITY UPLC System/XEVO-TQS; Waters; http://www.waters.com; Kojima et al., 2009; Kojima and Sakakibara, 2012).

Acknowledgements

We thank H. Teshima, R. Soga and K.-i. Ichikawa (University of Tokyo, Japan) for their assistance in cultivating rice plants at the Experimental Farm of the University of Tokyo. We also thank Dr T. Kawakatsu and Dr Y. Sato (University of Tokyo, Japan) for the initial studies of the *pre* mutant.

Competing interests

The authors declare no competing or financial interests.

Author contributions

K.-i.H., J.-i.I. and Y.N. designed experiments. K.-i.H. and M.I. carried out the majority of the experiments. K.-i.H., M.I., M.M., N.S., M.K., H.S. and T.Y. carried out experiments, analyzed and interpreted data. K.-i.H., Y.K. and Y.N. wrote the paper. All authors read and commented on the manuscript prior to submission.

Funding

This work was supported in part by Grants-in-Aid for Scientific Research from the Ministry of Education, Culture, Sports, Science, and Technology of Japan [23658005 to Y.N. and K.-i.H. and 24380005 to J.-i.I.].

Data availability

Sequence data for *PRE* (*OsAOS1*) (*Os03g0767000*) complete cDNA and protein can be found in the GenBank data libraries under accession number LC163980 (available at: https://www.ncbi.nlm.nih.gov/nuccore/LC163980).

Supplementary information

Supplementary information available online at
http://dev.biologists.org/lookup/doi/10.1242/dev.138602.supplemental

References

Asai, K., Satoh, N., Sasaki, H., Satoh, H. and Nagato, Y. (2002). A rice heterochronic mutant, mori1, is defective in the juvenile-adult phase change. *Development* **129**, 265-273.

Aukerman, M. J. and Sakai, H. (2003). Regulation of flowering time and floral organ identity by a MicroRNA and its APETALA2-like target genes. *Plant Cell* **15**, 2730-2741.

Axtell, M. J. and Bowman, J. L. (2008). Evolution of plant microRNAs and their targets. *Trends Plant Sci.* **13**, 343-349.

Beydler, B., Osadchuk, K., Cheng, C.-L., Manak, J. R. and Irish, E. E. (2016). The juvenile phase of maize sees upregulation of stress-response genes and is extended by exogenous jasmonic acid. *Plant Physiol.* **171**, 2648-2658.

Bollman, K. M., Aukerman, M. J., Park, M.-Y., Hunter, C., Berardini, T. Z. and Poethig, R. S. (2003). HASTY, the *Arabidopsis* ortholog of exportin 5/MSN5, regulates phase change and morphogenesis. *Development* **130**, 1493-1504.

Cai, Q., Yuan, Z., Chen, M., Yin, C., Luo, Z., Zhao, X., Liang, W., Hu, J. and Zhang, D. (2014). Jasmonic acid regulates spikelet development in rice. *Nat. Commun.* **5**, 3476.

Caldelari, D., Wang, G., Farmer, E. E. and Dong, X. (2011). Arabidopsis lox3 lox4 double mutants are male sterile and defective in global proliferative arrest. *Plant Mol. Biol.* **75**, 25-33.

Chen, X. (2004). A microRNA as a translational repressor of APETALA2 in Arabidopsis flower development. *Science* **303**, 2022-2025.

Chuck, G., Cigan, A. M., Saeteurn, K. and Hake, S. (2007). The heterochronic maize mutant Corngrass1 results from overexpression of a tandem microRNA. *Nat. Genet.* **39**, 544-549.

Chuck, G. S., Tobias, C., Sun, L., Kraemer, F., Li, C., Dibble, D., Arora, R., Bragg, J. N., Vogel, J. P., Singh, S. et al. (2011). Overexpression of the maize Corngrass1 microRNA prevents flowering, improves digestibility, and increases starch content of switchgrass. *Proc. Natl. Acad. Sci. USA* **108**, 17550-17555.

Evans, M. M. S. and Poethig, R. S. (1995). Gibberellins promote vegetative phase change and reproductive maturity in maize. *Plant Physiol.* **108**, 475-487.

Franco-Zorrilla, J. M., Valli, A., Todesco, M., Mateos, I., Puga, M. I., Rubio-Somoza, I., Leyva, A., Weigel, D., García, J. A. and Paz-Ares, J. (2007). Target mimicry provides a new mechanism for regulation of microRNA activity. *Nat. Genet.* **39**, 1033-1037.

Galvão, V. C., Horrer, D., Küttner, F. and Schmid, M. (2012). Spatial control of flowering by DELLA proteins in Arabidopsis thaliana. *Development* **139**, 4072-4082.

Haga, K. and Iino, M. (2004). Phytochrome-mediated transcriptional up-regulation of ALLENE OXIDE SYNTHASE in rice seedlings. *Plant Cell Physiol.* **45**, 119-128.

Hirochika, H. (2001). Contribution of the Tos17 retrotransposon to rice functional genomics. *Curr. Opin. Plant Biol.* **4**, 118-122.

Hirochika, H., Sugimoto, K., Otsuki, Y., Tsugawa, H. and Kanda, M. (1996). Retrotransposons of rice involved in mutations induced by tissue culture. *Proc. Natl. Acad. Sci. USA* **93**, 7783-7788.

Hou, X., Lee, L. Y. C., Xia, K., Yan, Y. and Yu, H. (2010). DELLAs modulate jasmonate signaling via competitive binding to JAZs. *Dev. Cell* **19**, 884-894.

Hudson, C. J., Freeman, J. S., Jones, R. C., Potts, B. M., Wong, M. M. L., Weller, J. L., Hecht, V. F. G., Poethig, R. S. and Vaillancourt, R. E. (2014). Genetic control of heterochrony in Eucalyptus globulus. *G3* **4**, 1235-1245.

Hunter, C., Sun, H. and Poethig, R. S. (2003). The Arabidopsis heterochronic gene ZIPPY is an ARGONAUTE family member. *Curr. Biol.* **13**, 1734-1739.

Ishiguro, S., Kawai-Oda, A., Ueda, J., Nishida, I. and Okada, K. (2001). The DEFECTIVE IN ANTHER DEHISCENCE1 gene encodes a novel phospholipase A1 catalyzing the initial step of jasmonic acid biosynthesis, which synchronizes pollen maturation, anther dehiscence, and flower opening in Arabidopsis. *Plant Cell* **13**, 2191-2209.

Itoh, J.-I., Hasegawa, A., Kitano, H. and Nagato, Y. (1998). A recessive heterochronic mutation, plastochron1, shortens the plastochron and elongates the vegetative phase in rice. *Plant Cell* **10**, 1511-1522.

Itoh, J.-I., Nonomura, K.-I., Ikeda, K., Yamaki, S., Inukai, Y., Yamagishi, H., Kitano, H. and Nagato, Y. (2005). Rice plant development: from zygote to spikelet. *Plant Cell Physiol.* **46**, 23-47.

Jung, J.-H., Seo, Y.-H., Seo, P. J., Reyes, J. L., Yun, J., Chua, N.-H. and Park, C.-M. (2007). The GIGANTEA-regulated microRNA172 mediates photoperiodic flowering independent of CONSTANS in Arabidopsis. *Plant Cell* **19**, 2736-2748.

Jung, J.-H., Ju, Y., Seo, P. J., Lee, J.-H. and Park, C.-M. (2012). The SOC1-SPL module integrates photoperiod and gibberellic acid signals to control flowering time in Arabidopsis. *Plant J.* **69**, 577-588.

Kawakatsu, T., Itoh, J., Miyoshi, K., Kurata, N., Alvarez, N., Veit, B. and Nagato, Y. (2006). PLASTOCHRON2 regulates leaf initiation and maturation in rice. *Plant Cell* **18**, 612-625.

Kojima, M. and Sakakibara, H. (2012). Highly sensitive high-throughput profiling of six phytohormones using MS-probe modification and liquid chromatography–tandem mass spectrometry. *Methods Mol. Biol.* **918**, 151-164.

Kojima, M., Kamada-Nobusada, T., Komatsu, H., Takei, K., Kuroha, T., Mizutani, M., Ashikari, M., Ueguchi-Tanaka, M., Matsuoka, M., Suzuki, K. et al. (2009). Highly sensitive and high-throughput analysis of plant hormones using MS-probe modification and liquid chromatography-tandem mass spectrometry: an application for hormone profiling in Oryza sativa. *Plant Cell Physiol.* **50**, 1201-1214.

Kouchi, H. and Hata, S. (1993). Isolation and characterization of novel nodulin cDNAs representing genes expressed at early stages of soybean nodule development. *Mol. Gen. Genet.* **238**, 106-119.

Lauter, N., Kampani, A., Carlson, S., Goebel, M. and Moose, S. P. (2005). microRNA172 down-regulates glossy15 to promote vegetative phase change in maize. *Proc. Natl. Acad. Sci. USA* **102**, 9412-9417.

Li, S., Yang, X., Wu, F. and He, Y. (2012). HYL1 controls the miR156-mediated juvenile phase of vegetative growth. *J. Exp. Bot.* **63**, 2787-2798.

Marin, E., Jouannet, V., Herz, A., Lokerse, A. S., Weijers, D., Vaucheret, H., Nussaume, L., Crespi, M. D. and Maizel, A. (2010). miR390, *Arabidopsis*

TAS3 tasiRNAs, and their *AUXIN RESPONSE FACTOR* targets define an autoregulatory network quantitatively regulating lateral root growth. *Plant Cell* **22**, 1104-1117.
Mimura, M., Nagato, Y. and Itoh, J.-I. (2012). Rice PLASTOCHRON genes regulate leaf maturation downstream of the gibberellin signal transduction pathway. *Planta* **235**, 1081-1089.
Miyoshi, K., Ahn, B.-O., Kawakatsu, T., Ito, Y., Itoh, J.-I., Nagato, Y. and Kurata, N. (2004). PLASTOCHRON1, a timekeeper of leaf initiation in rice, encodes cytochrome P450. *Proc. Natl. Acad. Sci. USA* **101**, 875-880.
Moose, S. P. and Sisco, P. H. (1994). Glossy15 controls the epidermal juvenile-to-adult phase transition in maize. *Plant Cell* **6**, 1343-1355.
Murashige, T. and Skoog, F. (1962). A revised medium for rapid growth and bio assays with tobacco tissue cultures. *Physiol. Plant.* **15**, 473-497.
Navarro, L., Bari, R., Achard, P., Lisón, P., Nemri, A., Harberd, N. P. and Jones, J. D. G. (2008). DELLAs control plant immune responses by modulating the balance of jasmonic acid and salicylic acid signaling. *Curr. Biol.* **18**, 650-655.
Noir, S., Bömer, M., Takahashi, N., Ishida, T., Tsui, T.-L., Balbi, V., Shanahan, H., Sugimoto, K. and Devoto, A. (2013). Jasmonate controls leaf growth by repressing cell proliferation and the onset of endoreduplication while maintaining a potential stand-by mode. *Plant Physiol.* **161**, 1930-1951.
Orkwiszewski, J. A. J. and Poethig, R. S. (2000). Phase identity of the maize leaf is determined after leaf initiation. *Proc. Natl. Acad. Sci. USA* **97**, 10631-10636.
Ozawa, K. (2012). A high-efficiency *Agrobacterium*-mediated transformation system of rice (*Oryza sativa L.*). *Methods Mol. Biol.* **847**, 51-57.
Park, J.-H., Halitschke, R., Kim, H. B., Baldwin, I. T., Feldmann, K. A. and Feyereisen, R. (2002). A knock-out mutation in allene oxide synthase results in male sterility and defective wound signal transduction in *Arabidopsis* due to a block in jasmonic acid biosynthesis. *Plant J.* **31**, 1-12.
Poethig, R. S. (2013). Chapter five – vegetative phase change and shoot maturation in plants. *Curr. Top. Dev. Biol.* **105**, 125-152.
Riemann, M., Müller, A., Korte, A., Furuya, M., Weiler, E. W. and Nick, P. (2003). Impaired induction of the jasmonate pathway in the rice mutant *hebiba*. *Plant Physiol.* **133**, 1820-1830.
Riemann, M., Haga, K., Shimizu, T., Okada, K., Ando, S., Mochizuki, S., Nishizawa, Y., Yamanouchi, U., Nick, P., Yano, M. et al. (2013). Identification of rice *Allene Oxide Cyclase* mutants and the function of jasmonate for defence against *Magnaporthe oryzae*. *Plant J.* **74**, 226-238.
Rogler, C. E. and Hackett, W. P. (1975). Phase change in hedera helix: induction of the mature to juvenile phase change by gibberellin A3. *Physiol. Plant.* **34**, 141-147.
Santino, A., Taurino, M., De Domenico, S., Bonsegna, S., Poltronieri, P., Pastor, V. and Flors, V. (2013). Jasmonate signaling in plant development and defense response to multiple (a)biotic stresses. *Plant Cell Rep.* **32**, 1085-1098.
Sato, Y., Antonio, B. A., Namiki, N., Takehisa, H., Minami, H., Kamatsuki, K., Sugimoto, K., Shimizu, Y., Hirochika, H. and Nagamura, Y. (2011). RiceXPro: a platform for monitoring gene expression in japonica rice grown under natural field conditions. *Nucleic Acids Res.* **39** Suppl. 1, D1141-D1148.
Schwab, R., Palatnik, J. F., Riester, M., Schommer, C., Schmid, M. and Weigel, D. (2005). Specific effects of microRNAs on the plant transcriptome. *Dev. Cell* **8**, 517-527.
Smith, M. R., Willmann, M. R., Wu, G., Berardini, T. Z., Möller, B., Weijers, D. and Poethig, R. S. (2009). Cyclophilin 40 is required for microRNA activity in Arabidopsis. *Proc. Natl. Acad. Sci. USA* **106**, 5424-5429.
Tanaka, N., Itoh, H., Sentoku, N., Kojima, M., Sakakibara, H., Izawa, T., Itoh, J.-I. and Nagato, Y. (2011). The *COP1* ortholog *PPS* regulates the juvenile–adult and vegetative–reproductive phase changes in rice. *Plant Cell* **23**, 2143-2154.
Telfer, A. and Poethig, R. S. (1998). HASTY: a gene that regulates the timing of shoot maturation in Arabidopsis thaliana. *Development* **125**, 1889-1898.
Telfer, A., Bollman, K. M. and Poethig, R. S. (1997). Phase change and the regulation of trichome distribution in Arabidopsis thaliana. *Development* **124**, 645-654.
Todesco, M., Rubio-Somoza, I., Paz-Ares, J. and Weigel, D. (2010). A collection of target mimics for comprehensive analysis of microRNA function in Arabidopsis thaliana. *PLoS Genet.* **6**, e1001031.
Vanstraelen, M. and Benková, E. (2012). Hormonal interactions in the regulation of plant development. *Annu. Rev. Cell Dev. Biol.* **28**, 463-487.
von Malek, B., van der Graaff, E., Schneitz, K. and Keller, B. (2002). The Arabidopsis male-sterile mutant dde2-2 is defective in the ALLENE OXIDE SYNTHASE gene encoding one of the key enzymes of the jasmonic acid biosynthesis pathway. *Planta* **216**, 187-192.
Wang, J.-W., Czech, B. and Weigel, D. (2009). miR156-regulated SPL transcription factors define an endogenous flowering pathway in Arabidopsis thaliana. *Cell* **138**, 738-749.
Wang, J.-W., Park, M. Y., Wang, L.-J., Koo, Y., Chen, X.-Y., Weigel, D. and Poethig, R. S. (2011). miRNA control of vegetative phase change in trees. *PLoS Genet.* **7**, e1002012.
Wild, M., Daviére, J. M., Cheminant, S., Regnault, T., Baumberger, N., Heintz, D., Baltz, R., Genschik, P. and Achard, P. (2012). The Arabidopsis DELLA RGA-LIKE3 is a direct target of MYC2 and modulates jasmonate signaling responses. *Plant Cell* **24**, 3307-3319.
Wu, G. and Poethig, R. S. (2006). Temporal regulation of shoot development in *Arabidopsis thaliana* by *miR156* and its target *SPL3*. *Development* **133**, 3539-3547.
Wu, G., Park, M. Y., Conway, S. R., Wang, J.-W., Weigel, D. and Poethig, R. S. (2009). The sequential action of miR156 and miR172 regulates developmental timing in Arabidopsis. *Cell* **138**, 750-759.
Xie, K., Wu, C. and Xiong, L. (2006). Genomic organization, differential expression, and interaction of SQUAMOSA promoter-binding-like transcription factors and microRNA156 in rice. *Plant Physiol.* **142**, 280-293.
Xie, K., Shen, J., Hou, X., Yao, J., Li, X., Xiao, J. and Xiong, L. (2012). Gradual increase of miR156 regulates temporal expression changes of numerous genes during leaf development in rice. *Plant Physiol.* **158**, 1382-1394.
Yang, L., Wu, G. and Poethig, R. S. (2012). Mutations in the GW-repeat protein SUO reveal a developmental function for microRNA-mediated translational repression in Arabidopsis. *Proc. Natl. Acad. Sci. USA* **109**, 315-320.
Yang, L., Xu, M., Koo, Y., He, J. and Poethig, R. S. (2013). Sugar promotes vegetative phase change in Arabidopsis thaliana by repressing the expression of MIR156A and MIR156C. *eLife* **2**, e00260.
Yoshikawa, T., Ozawa, S., Sentoku, N., Itoh, J.-I., Nagato, Y. and Yokoi, S. (2013). Change of shoot architecture during juvenile-to-adult phase transition in soybean. *Planta* **238**, 229-237.
Yu, S., Galvão, V. C., Zhang, Y.-C., Horrer, D., Zhang, T.-Q., Hao, Y.-H., Feng, Y.-Q., Wang, S., Schmid, M. and Wang, J.-W. (2012). Gibberellin regulates the Arabidopsis floral transition through miR156-targeted SQUAMOSA promoter binding-like transcription factors. *Plant Cell* **24**, 3320-3332.
Yu, S., Cao, L., Zhou, C.-M., Zhang, T.-Q., Lian, H., Sun, Y., Wu, J., Huang, J., Wang, G. and Wang, J.-W. (2013). Sugar is an endogenous cue for juvenile-to-adult phase transition in plants. *eLife* **2**, e00269.
Yuan, Z. and Zhang, D. (2015). Roles of jasmonate signalling in plant inflorescence and flower development. *Curr. Opin. Plant Biol.* **27**, 44-51.
Zhang, X., Zou, Z., Zhang, J., Zhang, Y., Han, Q., Hu, T., Xu, X., Liu, H., Li, H. and Ye, Z. (2011). Over-expression of sly-miR156a in tomato results in multiple vegetative and reproductive trait alterations and partial phenocopy of the *sft* mutant. *FEBS Lett.* **585**, 435-439.
Zuo, J., Zhu, B., Fu, D., Zhu, Y., Ma, Y., Chi, L., Ju, Z., Wang, Y., Zhai, B. and Luo, Y. (2012). Sculpting the maturation, softening and ethylene pathway: the influences of microRNAs on tomato fruits. *BMC Genomics* **13**, 7.

Supplementary Material

Supplementary Figures and Tables

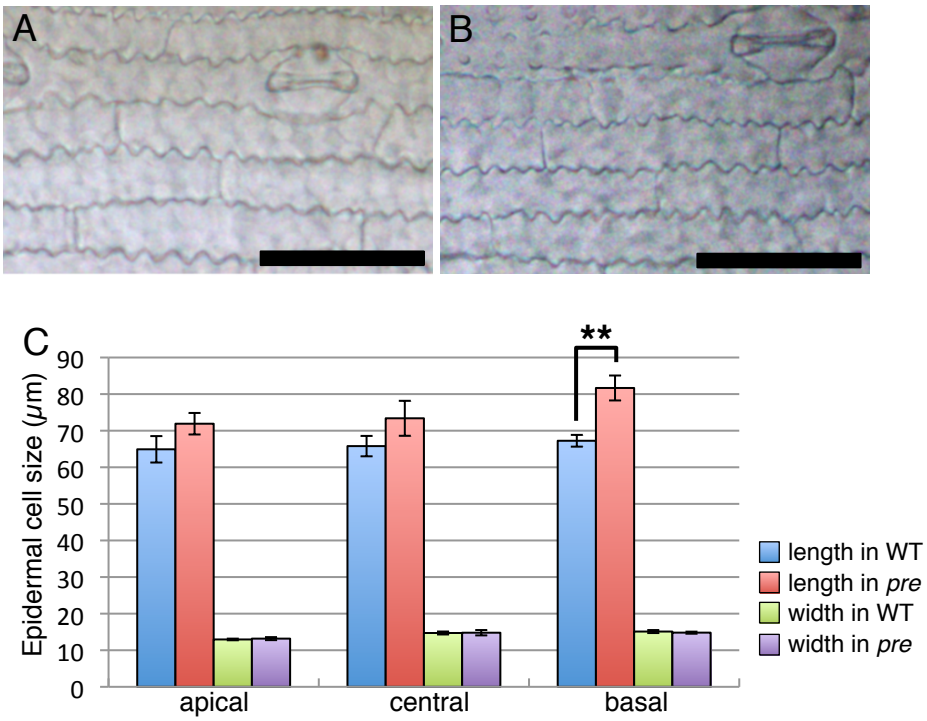

Fig. S1. Comparison of epidermal cell size between wild type and *pre*.
(A, B) Epidermal cells in the basal region of the second leaf blade in wild type (A) and *pre* (B). Scale bars = 5 µm. (C) Comparison of epidermal cell sizes in apical, central and basal regions of the second leaf blade in wild type and *pre* ($n \geqq 10$) . Data are shown as means ± s.e.m. ** = $P < 0.01$ (Student's *t*-test).

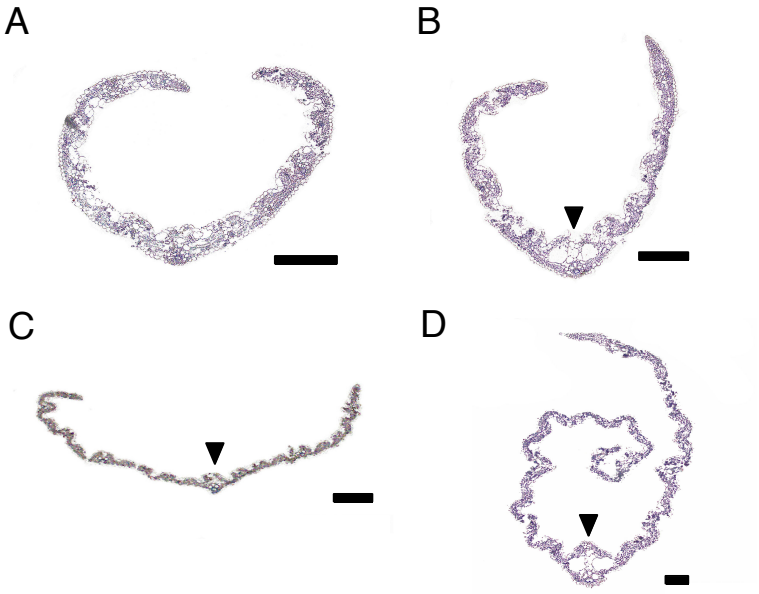

Fig. S2. Cross-sections of leaf blade in wild type and *pre*.
(A) Cross section of wild-type second leaf blade cut at 8 % from the base to the tip. (B) Cross section of *pre* second leaf blade cut at 22 % from the base. (C) Cross section of wild-type third leaf blade cut at 50 % from the base. (D) Cross section of *pre* third leaf blade cut at 60 % from the base. Arrowheads indicate midribs. Scale bars = 100 µm in (A, B) and 200 µm in (C, D).

Development • Supplementary information

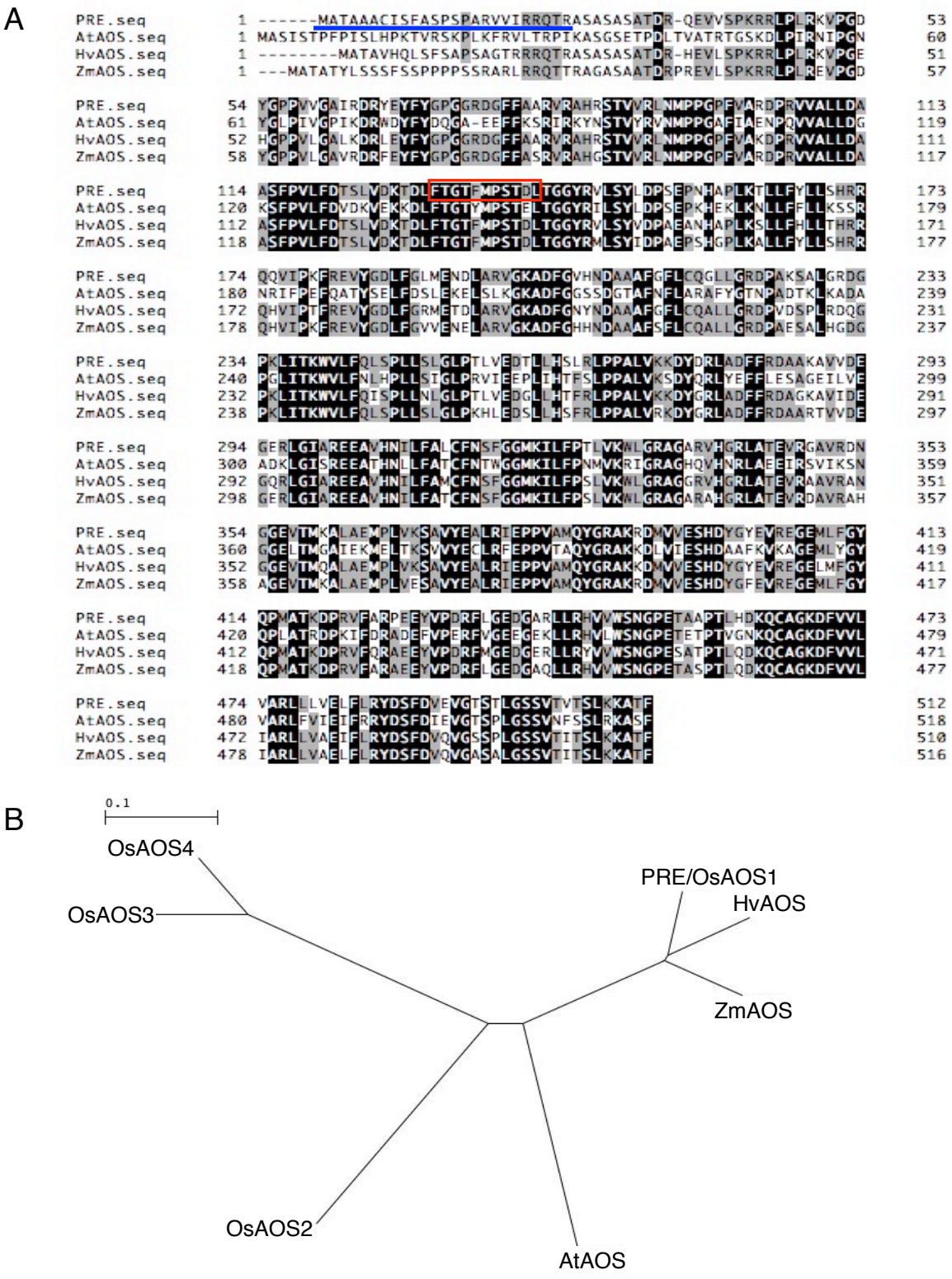

Figure S3. Alignments of amino acid sequences and the phylogenetic tree of PRE/AOS proteins.
(A) Alignment of deduced amino acid sequences of PRE protein and three AOS proteins from arabidopsis (At), barley (Hv) and maize (Zm). Blue underline indicates a chloroplast transit peptide. Deletion site in *pre* is indicated as a red box. Residues conserved in all four proteins are shaded in black, and those conserved in three proteins are shaded in grey.
(B) The phylogenetic tree of PRE/AOS proteins from rice (Os), arabidopsis (At), barley (Hv) and maize (Zm) constructed by the neighbor-joining method. The bootstrap values based on 1000 replicates are shown as the numbers.

Development • Supplementary information

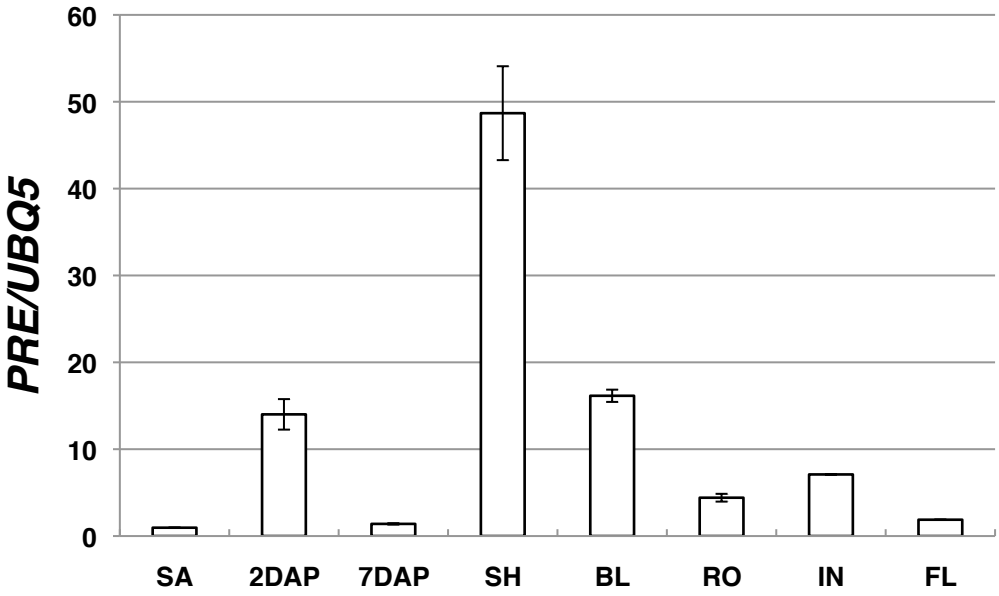

Fig. S4. Expression profile of *PRE* gene.
qPCR analysis of *PRE* gene expression in wild-type tissues including shoot apex at 14 days after sowing (SA), ovary at 2 or 7 days after pollination (2 DAP and 7 DAP), the third leaf sheath (SH), the third leaf blade (BL), root (RO), young panicle at the primary rachis branch differentiation stage (IN) and flower (FL). *OsUBQ5* was used as an internal control. Values are shown as means of three technical replicates ±s.d.

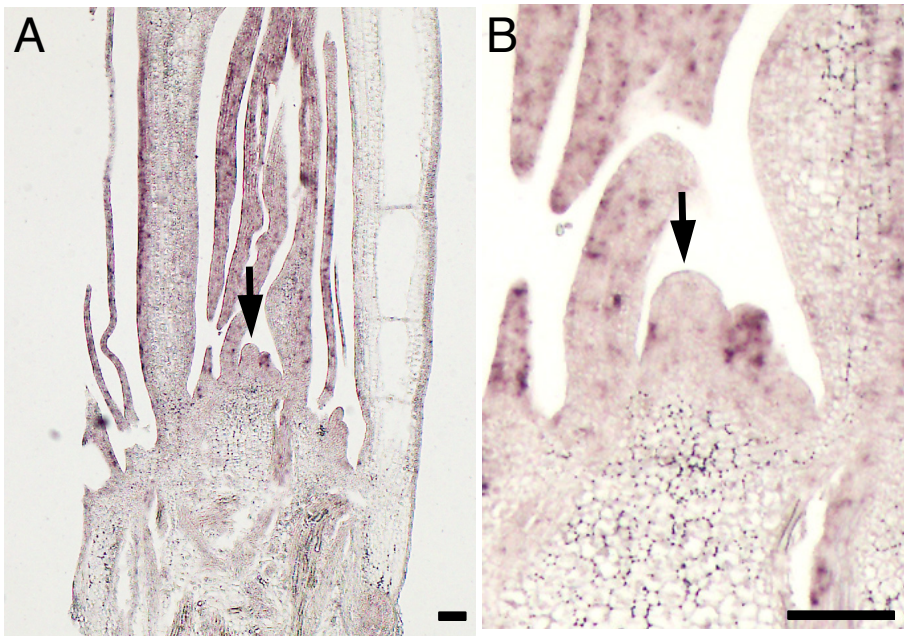

Fig. S5. *in situ* hybridization using *PRE* sense probe.
(A) Expression pattern in 14 day-old wild type shoot apex when *PRE* sense probe was used. (B) Magnified view of shoot apex in (A). Accumulation of complementary mRNA to *PRE* mRNA implies the expression of *Os03t0766900-02* transcripts (Figure 3). Arrows indicate shoot apical meristems. Scale bars = 100 µm.

Development • Supplementary information

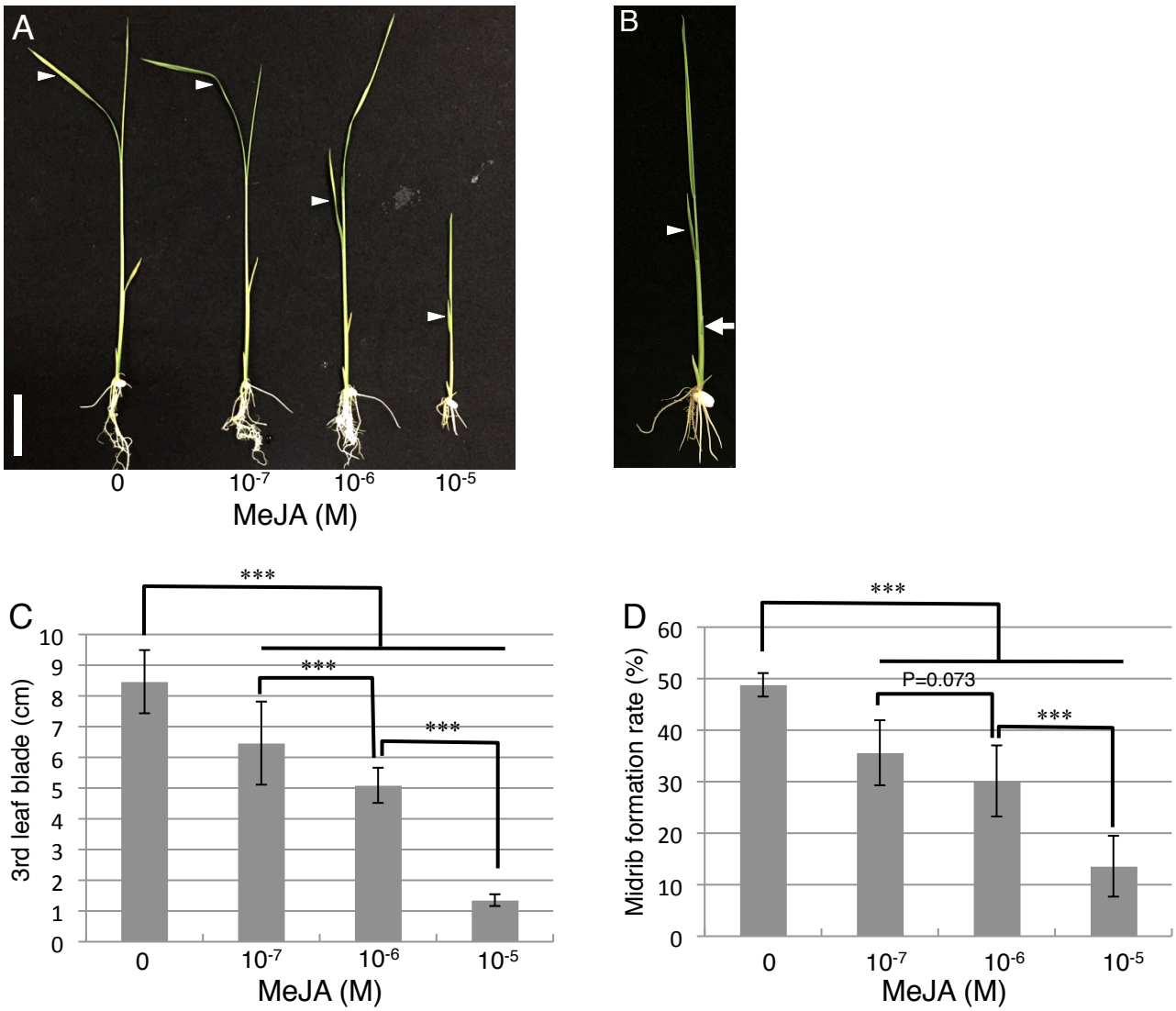

Fig. S6. Effect of JA on leaf length and midrib formation

(A) Wild-type seedlings in 13 days after germination on the medium containing different concentrations of MeJA. Arrowheads indicate the third leaves. Scale bar = 3cm. (B) Higher magnification of the seedling grown on the medium containing 10^{-5}M MeJA in (A). Arrow indicates the second leaf.
(C) Comparison of the third leaf blade on the medium containing different concentrations of MeJA. ($n \geqq 10$). (D) The percentage of midrib length against total leaf blade length in 3rd leaf blades ($n \geqq 10$) . Data are shown as means ±SD. ***= $P < 0.001$ (Student's *t*-test).

Development • Supplementary information

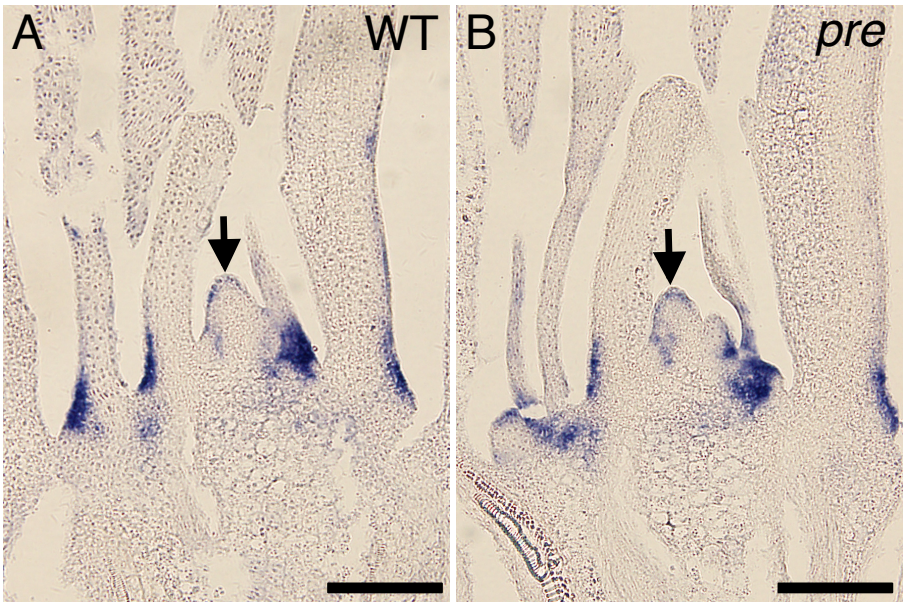

Fig. S7. *in* situ hybridization analysis of *PLA1* in wild type and *pre*.
(A, B) Longitudinal sections of 10-day-old shoot apices in wild type (A) and *pre* (B). Arrows indicate shoot apical meristems. Scale bars = 200 µm.

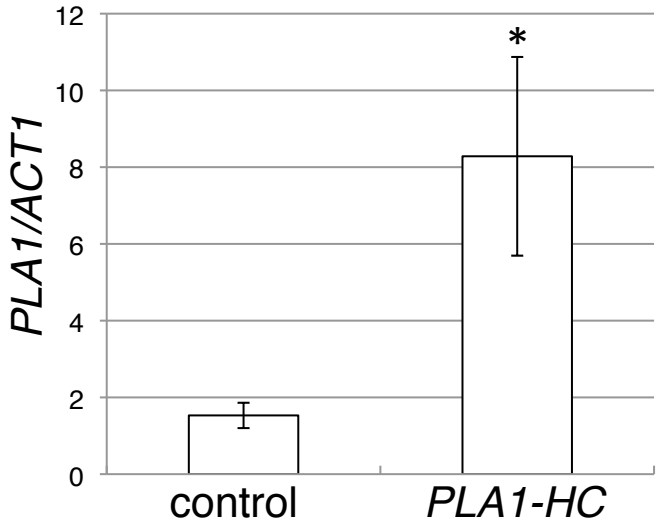

Fig. S8. Expression of *PLA1* in *PLA1-HC*.
Expression level of *PLA1* in the control and *PLA1-HC* shoot apices. Expression level was normalized by that of *OsACTIN1*(*ACT1*). The data shown are as means of three biological replicates ±SD. **P* <0.05 (Student's *t*-test).

Development • Supplementary information

Table S1. Primer sequence used for the experiment

Primers for Mapping

name	Marker type	Forward Primer	Reverse Primer
K0437	Direct sequence	ctgttgatgctggcgtttt	tttgcccatcacgactatga
0079B15	SSLP	ggacttcacttaggttgtgt	gctcgatgttccagtcaagt
K0320	CAPS(PstI)	tgtgtgcccgtctatggaat	agtttatcgccatggtcctg
K0011	CAPS(MboI)	acttttgcttcggagcagtg	tttgcgtttctgtttgaagga

Primers for RT-PCR

Transcrpts	Forward Primer (name)	Reverse Primer (name)
Os03t0766900-01,-02	cagaagatatgactggtgatc (F1)	cactagataggtcttcaagtc (R1)
Os03t0766900-02	gtggaattccaagctccaag (F2)	gcacatccacaaaactgcac (R2)
Os03t0767000-01	tcctccgatacgactccttc (F3)	tgatcacaccatacagagtga (R3)
OsACTIN1	tccatcttggcatctctcag	gtaccctcatcaggcatctg

Development • Supplementary information